Back to Session Subjects

Toward a bio-inspired non-emissive powerline detection system.

Stéphane Viollet, Jean Michelis and Nicolas Franceschini

Biorobotics research group, Movement and Perception Lab.,
CNRS / Univ. de la Méditerranée
31, chemin Joseph Aiguier, 13402 Marseille Cedex 20, FRANCE
e-mail: {stephane.viollet, jean.michelis, nicolas.franceschini}@univmed.fr

Key words: Scanning sensor, hyperacuity, non-emissive vision, insect vision.

We present here a proof-of–concept powerline detection system. Powerlines are the number one hazard for low-flying helicopters. Most of the detection systems available on the market tend to enlarge the operability time by detecting wires through fog, rain and snow. However, these systems need to emit radiations in the millimeter wave range (radar-based systems) or in the infrared range (laser-based systems) to detect an obstacle. This emissive sensing has a significant cost in terms of mass, size and money. The principle of the proposed powerline detection system was inspired by studies carried out at our laboratory on the compound eye of the fly. Unlike existing systems, our system does not emit any radiation. The first requirement for detecting a cable is that a retina, made of infrared sensitive photodiodes placed behind a lens, must *vibrate* actively and periodically according to a particular law inspired by the fly itself. The second requirement relies on the contrast value (at least 4%) of the object placed with the field-of-view. However, we show that the performance of our detection system is quasi-invariant with respect to contrast (from 4% to 70%). Our system is able to detect a thin bar, 0.3mm wide, at a distance of 10m and hence potentially a 30mm bar at 1km. Although not tested in real conditions, our system presents an interesting prospect for the development of a non-emissive powerline detection system when it comes to reduce the avionic mass, power consumption and cost.

INTRODUCTION

In spite of many programs launched in the last 20 years, the problem of helicopter wire-strikes is still a major issue. This problem is particularly acute during missions where flight profiles are below 100 meters or during maintenance operations where the pilot has to stabilize the helicopter a couple of meters away from powerlines. Most wire strikes do not occur only during these critical flight conditions but during daylight missions under relatively favorable weather conditions [1,2]. Scanning beam laser [1-7] or millimetric radar [8] systems exhibit high performances in terms of wire detection range and detection probability. For example, the HELLAS [3] system can detect a wire of 10mm diameter at a distance of 500m with a detection probability of 99.5%. Yet these emissive systems are bulky, heavy, costly and power hungry. Laser based systems consume between 300W and 600W and their mass is between 10kg and 30kg. Furthermore, microwave and millimeter wave radars suffer from specular reflections [8] but offer a better resolution image than laser based system in the presence of clouds, smoke and fog. Several detection systems [1] are based on joint emission of infrared and millimeter waves but this solution presents a very high cost. This work examines an alternative way to reduce the size, the mass and the cost of a powerline detection system.

The proposed system relies upon a principle that was discovered in the compound eye of the fly in 1997 [10]. Flying insects are equipped with one of the oldest optical sensor ever developped, the compound eye, which is one of the most complex in terms of micro-mechanical structure and optical alignment. If we make a comparaison with off-the-shelf optical sensor wich are currently used onboard UAV, aerial robots and helicopters, insects like flies or dragonflies must deal with a sensor having relatively few pixels, and consequently a low angular resolution. However, even the smallest fruitfly, *drosophila*, is able to avoid obstacles with high performances.

Since about 100 years, the visual system of the fly and especially its compound eye has fascinated many researchers [9]. A striking example of biomimetic transfer comes from studies on the Elementary Motion Detector (EMD) neurons, the mechanism of which has been analysed in flies with single neuron recordings and single photoreceptor stimulations [11] and reproduced electronically at our laboratory with SMD technology [12,14]. This EMD circuit is the keystone of the visual processing implemented in the proposed powerline detection system. In section 2, we recall the principle of the patented [13] *variable speed micro-scanner* which was firstly implemented onboard robotic platforms at our laboratory [15,16]. A complete description of the system and its performances is given in section 3.

1 PRINCIPLE OF THE DETECTION SYSTEM

Consider a classical imager composed of a matrix of elementary infrared receptors. In most of the cases, its resolution is not sufficient to detect contrasting objects such as remote wires, power cables, guide ropes and so on. In the system proposed here, the resolution is dramatically improved by imposing upon the photoreceptor array, a periodic micro-scanning movement. The principle of this detection system is based on findings made at our laboratory on a retinal scanning process that was observed in the compound eye of the fly [10]. In the next, we consider two neighbouring elements of the photoreceptor array. This photoreceptor pair thus defines one “cell” of the proposed powerline detection system.

2.1 Description of the detection system

Figure 1 depicts an elementary "eye" composed of a lens (focal length f) and two photoreceptors placed behind the lens. The (small) angular separation Δφ between the visual axes of these two receptors depends on the linear pitch *p* of the receptors and the focal length *f*:

$$\Delta\varphi = \frac{p}{f} \tag{1}$$

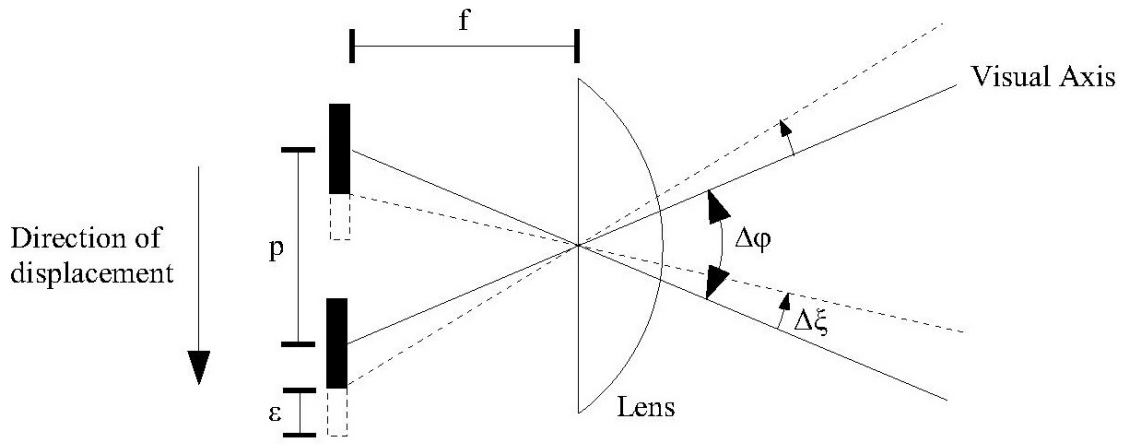

***Fig 1**. Illustation of the scanning principle. Here, a downward translation of the pair of photoreceptors by an elementary step ε produces an upward rotation of their visual axes by an angle $\Delta\xi$. The angle $\Delta\varphi$ is constant and depends simply on the focal length f and the pitch p of the photoreceptors (from [13]).*

Figure 1 shows that a downward displacement of the photoreceptors by an elementary step ε is equivalent to an angular rotation (here counterclockwise) of the visual axes by an elementary angle Δξ. In the configuration of figure 1, the lens is fixed and the sensor array translates. In an alternate configuration, the same angular rotation of the visual axes can be obtained by translating only the lens in front the fixed sensor array [13] or by rotating the whole eye (lens + photoreceptors) [15,16]. However, it turns out that it is more efficient to move the photoreceptor array than the optics, especially when heavy optical system are used. Thus, our scanning detection system can be seen as a system, the visual axes of which are rotating periodically at a frequency, an amplitude and a speed depending on the motion law which is imposed upon the photoreceptor array.

2.2 Simulation of a rotational scanning movement

Figure 2 presents the results of simulations experiments. The particular scanning mode, at a speed Ω(t) that varies with time is inspired by data on the retinal movements occurring in the compound eye of the fly [10]. The first phase of each retinal jerk Ψ(t) (which occurs at 5-10Hz in the flying fly) is an exponential function of time. The *speed* of the angular jerks is therefore an exponential function of time as well. In the same vein, the pair of photoreceptors

is assumed here to rotate clockwise at an angular speed $\Omega(t)$ which decays exponentially with time (fig 2b).

Figure 2 considers the concerted rotation of a photoreceptor pair, placed in front of an edge occupying 3 positions (indicated 1,2,3) along the x axis. For each of these stationary positions, Figures 2(c,d,e) give the output from photoreceptors 1 and 2 as they turn clockwise at the variable angular speed $\Omega(t)$. In Figures 2(f,g,h), the output from each photoreceptor was passed through an analog high-pass filter with a cut-off frequency of 20Hz. Each of the two filtered signals is seen to reach a threshold (dotted horizontal line) at instants separated by Δt.

The main result of this simulation is that the time lag Δt depends on the exact position (1,2,3) of the dark edge along the x axes. The reason for this effect is also shown in figure 2b: the edge placed at the beginning of the scan phase (position 1 in figure 2b) is seen to be detected at a higher speed than when it is in position 3.

We have chosen to use the angular sensitivity of an insect lens-photoreceptor system as an optical model of the eye. Unlike insects, in which spatial low-pass filtering naturally results from diffraction [17], a bell-shaped angular sensitivity can be easily achieved by defocusing the lens (decreasing the distance between the photoreceptor and the lens). The defocusing process has an important role as it permits:

- to smooth out the stiff temporal transitions generated by contrasting objects such as a dark edge (see figures 2c,d,e).
- to spatially low-pass filter the background and thus remove fine details which can be at the origin of false detections.

The following step consists in elaborating the visual processing required to measure the time lag Δt. The next section is a detailed description of a particular circuit called EMD circuit whose fonction is precisely to assess the time lag Δt.

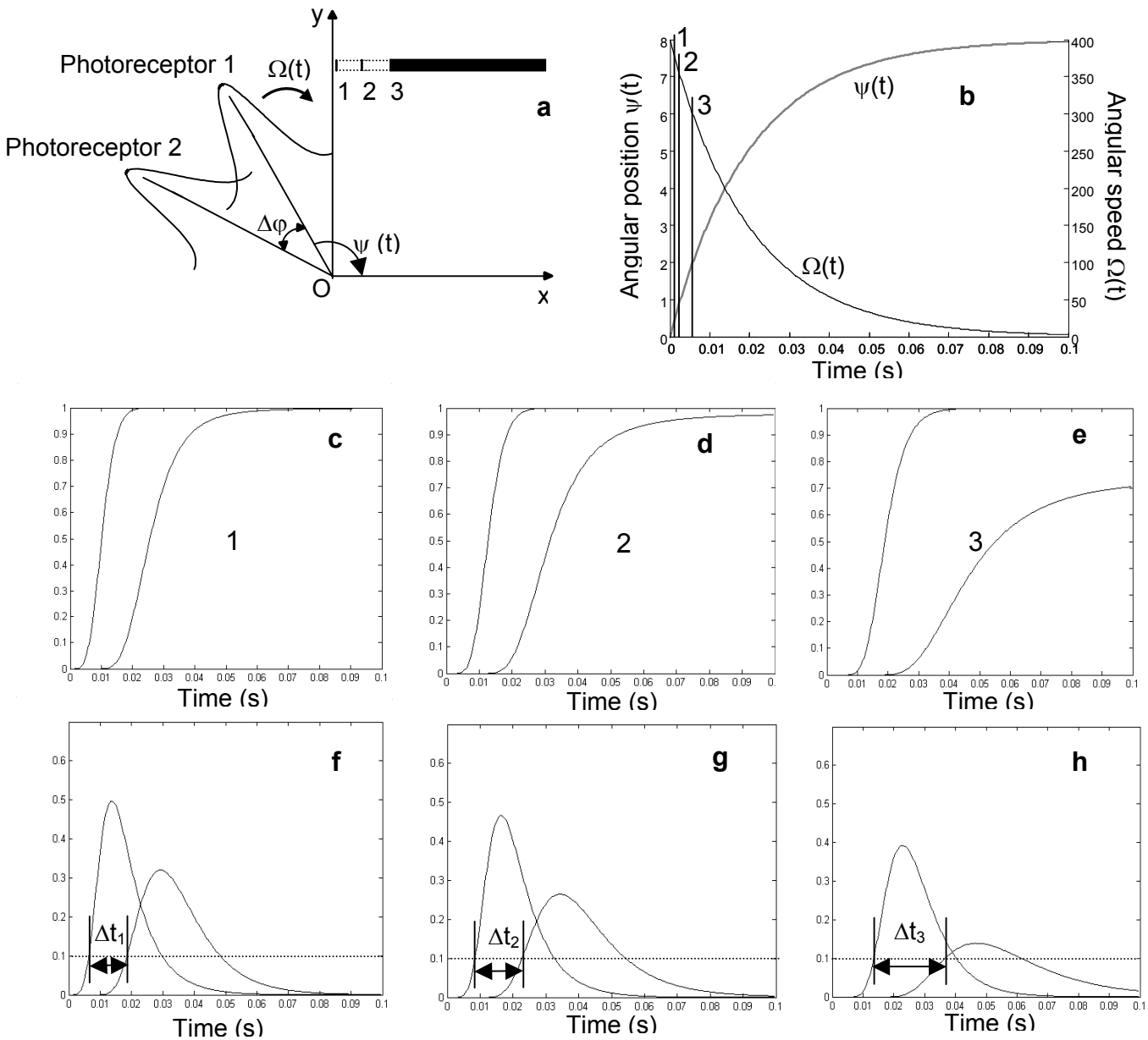

Fig. 2. *(a) Simulated response of a pair of adjacent photoreceptors (fig. 1) rotating clockwise at a variable angular speed $\Omega(t)$, and encountering a dark edge placed at various positions 1, 2, 3.*

(b) Exponential decrease of the angular speed $\Omega(t)$ and its integral, the angular position $\psi(t)$. The three vertical bars indicate for each position the exact moment at which the dark edge enters into the field-of-view (FOV) of photoreceptor 1.

(c, d, e) outputs of the two photoreceptors 1 and 2, depending of the position of the dark edge (1,2,3).

(f, g, h) high-pass filtered version of (c,d,e) (cutt-off frequency: 20Hz) and thresholding of the output signal from each photoreceptor: the time lag Δt happens to depend on the angular position 1,2,3 of the dark edge in the FOV. (from [15]).

2.3 Description of the visual processing steps

The original Elementary Motion Detector (EMD) is an analogue circuit producing an output signal that decreases as a function of the time lag Δt between its two inputs. As derived from an analysis of a motion detecting neuron in flies [11], the electronic analogue EMD is directionally selective and is able to distinguish between dark-to-light (ON contrast) and light-to-dark (OFF contrast) transitions. The signal processing scheme used in our EMD circuit is depicted in Fig. 3. It can be decomposed into 5 steps as follows:

- *Spatial* low-pass filtering is achieved by placing the photoreceptors between the focal plane and the lens (defocusing) (Fig. 2b). The cut-off spatial frequency depends on the amount of defocusing.
- High-pass *temporal* filtering of the signals in each channel cancels the DC component and discriminates between ON and OFF transitions.
- Low-pass *temporal* filtering reduces noise and interferences (e.g. 100-Hz interference originating from artificial lighting).
- Thresholding and pulse generation are performed on the signals in each channel for contrast detection.
- Time lag Δt, between the signals in the two channels, is measured by a counter.

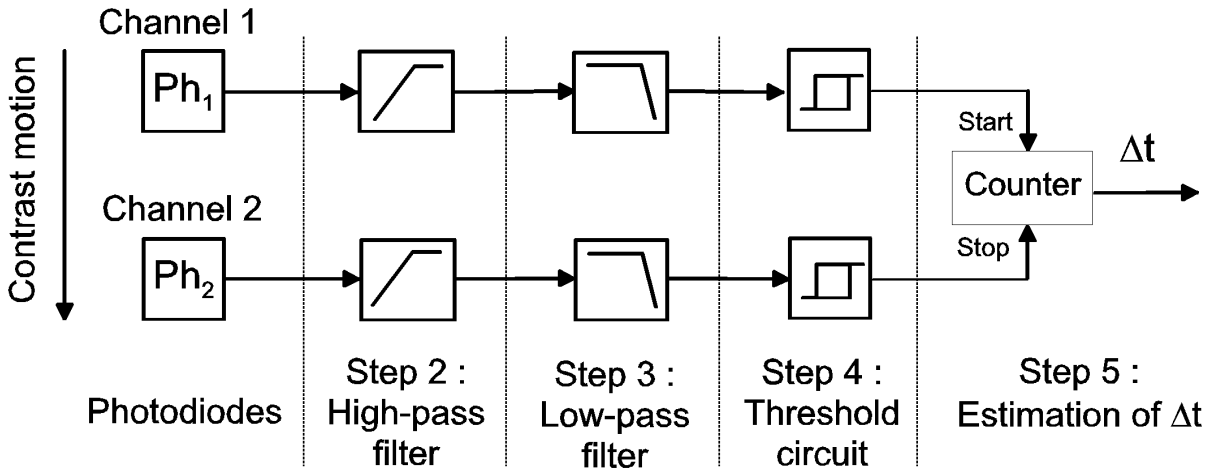

***Fig. 3**. Principle of the EMD circuit we constructed (after [11, 12, 14]). The fixed interreceptor angle Δφ (cf. figure 1) causes a temporal shift Δt between the two signals. In this non linear circuit, Δt happens to be fairly independent of contrast.*

3. THE PROOF OF CONCEPT DETECTION SYSTEM

3.1 Hardware implementation of the powerline detection system

Referring to the embodiment shown in figure 4, the elementary cell of the powerline detection system includes a lens (focal length 80mm), a photodiode array (from IC-Haus) and a piezo bimorph actuator (from Physik Instrumente). We installed an electrical and optical shield (not shown in figure 4) made of blackened aluminium plates on each side of the system.

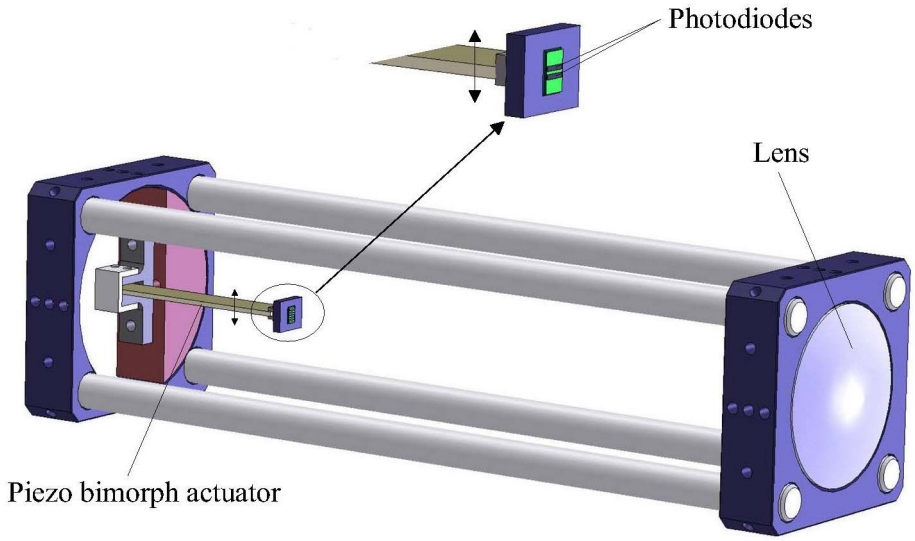

***Fig. 4**. Mock-up of the thin wire detection system with its "wiggling retina". The latter is composed of only two matched photodiodes (length 1.6mm, width 0.3mm, pitch 0.42mm) which are translated periodically at 10Hz (as suggested by the double arrows) near the focal plane of a stationary lens (diameter 30mm, focal length 80mm,) by means of a high resolution, high bandwidth piezo actuator. The latter is a multilayer piezoelectric bender giving a maximal deflection of 1 mm for an operating voltage of 60V.*

Each photodiode of the retina has an active area of 1600x300µm. Each photodiode's output drives its own integrated photocurrent amplifier, enabling good noise immunity to the analog output signal. Current-to-voltage conversion was achieved by a classical transimpedance amplifier. Saturation at high illuminances is prevented by installing a circular variable (logarithmic) neutral density filter (not shown here) between the lens and the photodiodes. This filter is part of a position servo-loop which makes the DC level of each photoreceptor's output relatively invariant with the mean luminance.

As described in section 2.2, the scanning law requires that during the first half of the scan cycle, the angular speed Ω must decay *exponentially* with time. The scanning cycle is completed by having the photodiodes return to their original position at a *constant* speed. All in all, we have therefore a two-phase micro-scanning movement :

- during phase (1) (duration: 50ms), the angular *speed* Ω(t) of the eye varies as a decreasing exponential function of time (Fig. 5). The angular *position* ψ(t) of the photodiodes' visual axes will therefore vary consequently as a saturating exponential function of time (see fig. 2b).

- during phase (2) (duration: 50ms), the angular orientations of the photodiodes' visual axes return to their original positions (Fig. 5) at a quasi-constant speed.

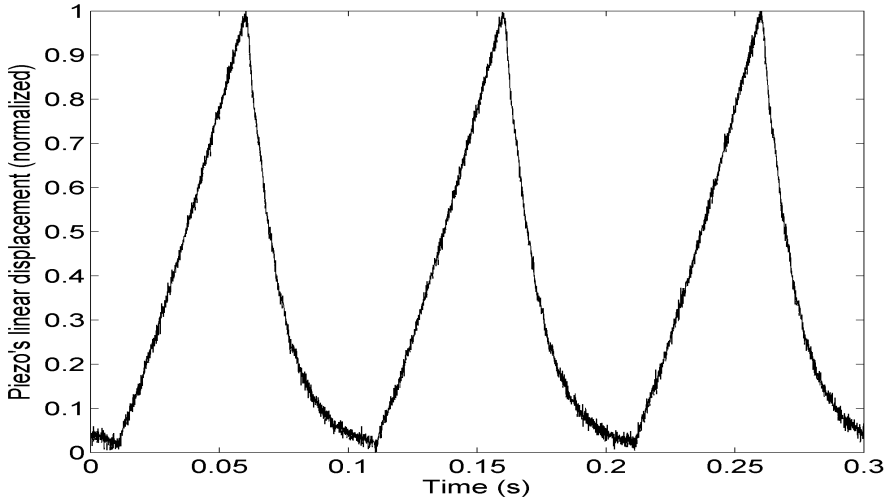

***Fig. 5**. Response of the piezo actuator to the particular scanning law (which translates the elementary retina see fig. 4) (scanning frequency 10Hz, maximum deflection of 1mm) as described in section 3.1. The displacement of the tip of the piezo is monitored here by a contactless magnetoresistive sensor that senses the movement of a miniature magnet (1mm^3) glued to the tip of the piezo.*

Figures 5 shows the linear position of the piezo that was measured by a contactless magnetoresistive sensor that sensed the displacement of a minature (0.1 gram) magnet glued at the tip of the piezo actuator. The two scanning phases (exponential and linear) described previously, are clearly distinguished. The high fidelity of the displacement shown in Figure 5 is due to the high bandwidth of the piezo bimorph actuator, which eliminates the need for any feedback loop, and hence simplifies the drive electronics.

Table 1 summarizes the main characteristics of the detection system.

Optics	Focal length: 80mm	F-Number: 2.66		
Photoreceptor	Pixel size: 800 x 300µm²	Pitch : 420µm	Photocurrent gain: 200	Bandwidth: 200kHz
Piezoelectric actuator	Dimensions: 39x12x0.65mm	Operating voltage: 0 – 60V	Deflection: ±450µm	Resonant frequency: 360Hz
Overall detection system	Supply voltage: ±12V	Supply current: < 200mA	$\Delta\varphi$:0,3°	Field of view ≈ 0.2°

***Table 1**. Main characteristics of the proof-of-concept powerline detection system.*

3.2 Performances

One of the main challenge of a powerline detection system is its ability to detect a thin elongated object at a great distance.We placed within the visual field of our detection system a thin bar (width 0.3mm 0.6 and 0.9mm) at a distance D equal to 10m. We changed the orientation of the line of sight of the detection system gradually in the vertical plane by applying a ramp composed of a miniature angular step displacements (amplitude one minute of arc, i.e., 0.015°). Figure 6 shows the signal output of the system versus the vertical angular position of the contrasting object with respect to the center of the visual field.

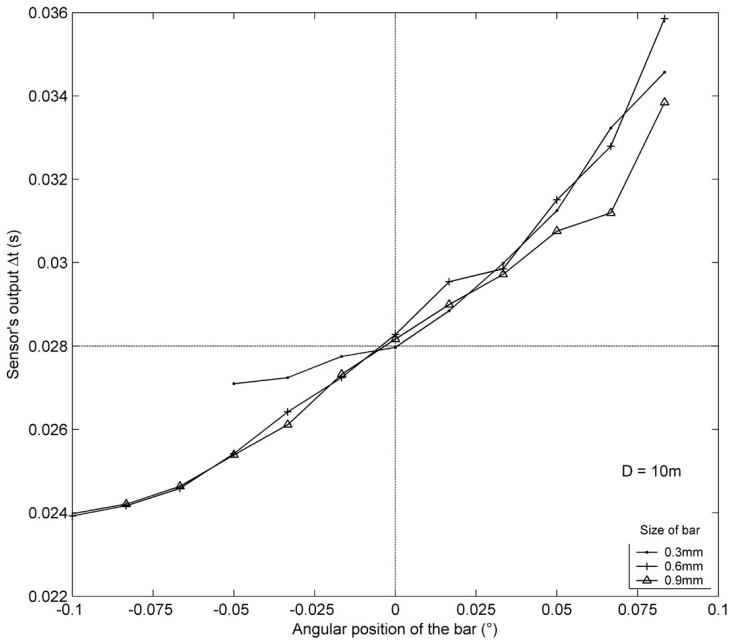

Fig.6 *Output signal of the detection system with respect to the angular position of a thin bar placed at different positions in its visual field. The detection system can locate a thin bar of 0.3mm wide (contrast 70%) with a resolution of about 0.01° (i.e, 30 times better than its static angular pitch $\Delta\varphi$ = 0.3°).*

Figure 6 shows that the proposed detection system is able to locate a thin bar (0.3mm wide) at a distance of 10m within its (0.2°) FOV. This is the minimum width of a bar that the detection system is able to detect. If we consider the detection range of 1km which is required by helicopter operators and if we neglect turbulences and other disturbances, our system could virtually detect a 30mm cable at 1km distance. Furthermore, figure 6 shows that the detection system is endowed with *hyperacuity* because it is able to locate the bar within its FOV with a resolution 30 times better than the static resolution imposed by the angle $\Delta\varphi$=0.3° (see figure 1).

A bar is not the only type of object that our system is able to detect. Figure 7 shows the response of the detection system to a *contrasting edge* placed in its visual field. Flying insects are equipped with particular sensors called *ocelli* whose function is precisely to locate a typical natural contrasting edge: the horizon. Insects use this visual information to stabilize their attitude arround the pitch and roll axes. The purpose is here to present the capacity of our system to detect and locate an edge with a high accuracy as well. It illustrates also the relative invariance of the detection system to a variation in contrast and its high sensitivity to low contrast (4%).

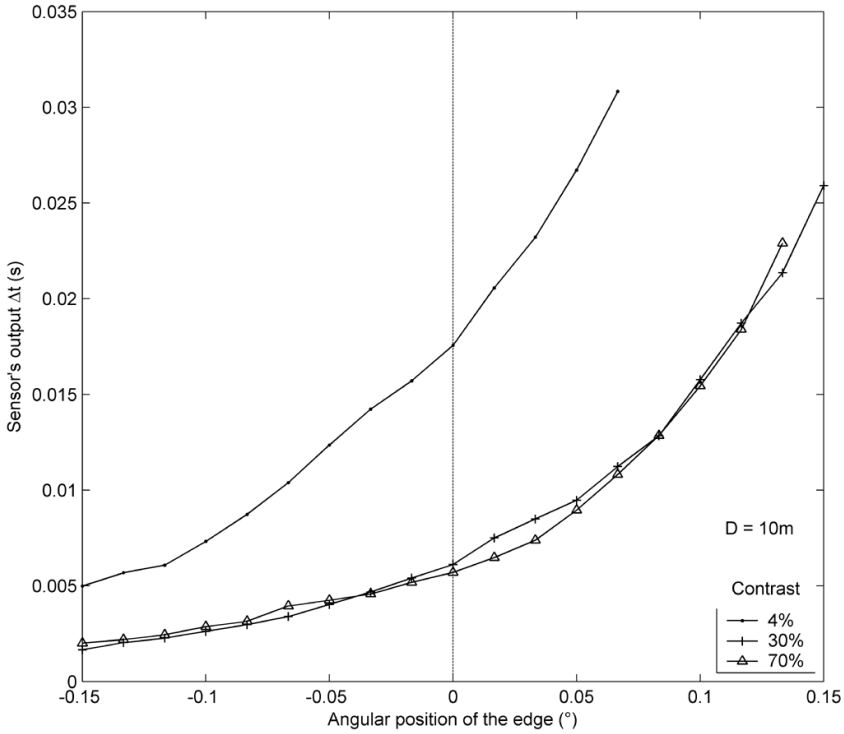

Fig.7 *Output signal of the detection system versus the angular position of the edge placed in its visual field. The system can locate a contrasting edge with the same resolution as a bar even if the edge contrast is as low as 4%.*

3.3 Discrimination between a bar and an edge

We have shown in previous sections that our elementary detection system is able to detect and locate contrasting edges or bars with a high accuracy, 30 times better than the resolution imposed by the optics. The signal processing steps of the EMD (cf. figure 3) does not give any knowledge about the nature of the object (bar or edge) seen by the detection system. The reliability of a powerline detection system is characterised by its probability to detect wires and thus, its ability to discriminate a wire from other objects (such as, e.g., the horizon). In this work, we also aimed at making the EMD described in section 2.3, selective to bars rather than edges. Figure 8 shows the new version of the EMD circuit.

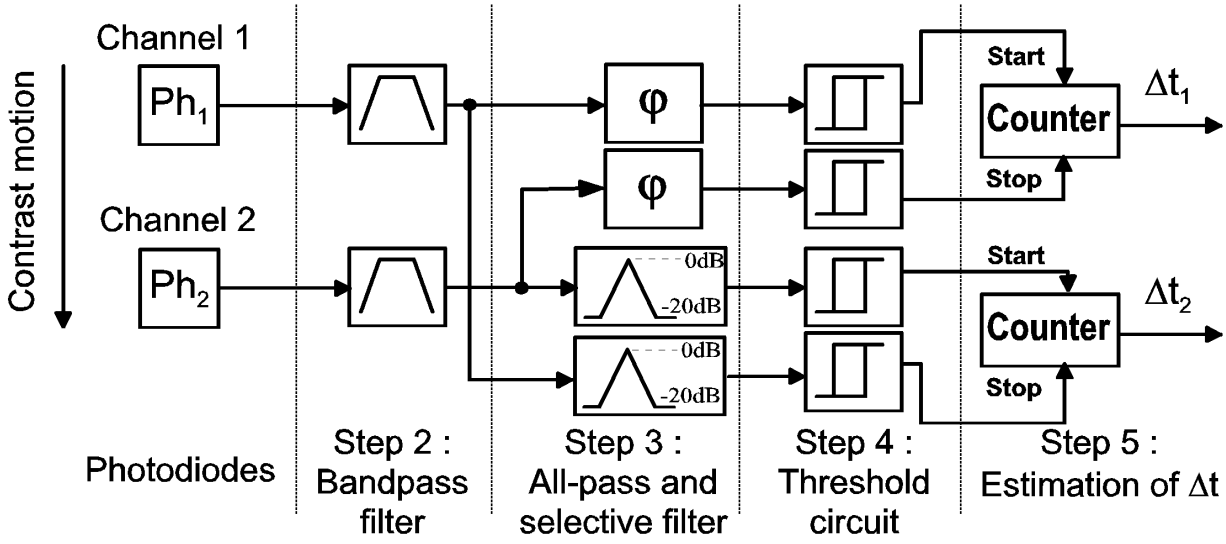

***Fig. 8**. Enhanced version of the EMD shown in figure 3. The additional processing steps (all-pass and selective filters) are used to yield two time-lag noted Δt_1 and Δt_2. The selective filters are centered arround the 10Hz scan frequency. In the case of an edge seen by the detection system, the fundamental frequency of the signal in channels 1 and 2 is 10Hz and thus, both Δt_1 and Δt_2 are available. But in the case of a bar, the fundamental frequency is 20Hz. Then, the amplitude of the selective filter's output signal is below the theshold and only Δt_1 is available.*

As described in section 3.1, the scanning frequency of the detection system is 10Hz. Whenever a contrasting edge is detected, the fundamental frequency of the signal in each visual pathway (called channels 1 and 2) will be also 10Hz because only one contrast transition is seen during a complete scan period. If a bar is detected, the fundamental frequency will be 20Hz. Thus, we can consider the following equation which links the spatial frequency with the temporal frequency of signal collected at the output of each photoreceptor :

$$f_t = nf_s \qquad (2)$$

with f_t the temporal frequency of the photereceptor's output signal, n the number of contrast transitions encountered during one scanning period and f_s the scanning frequency (here 10Hz).

Equation (2) reveals an important characteristic of the scanning process which transforms a spatial frequency into a temporal frequency. This property was originally formalized by Landolt *et al.* [19] on the basis of studies on retinal movements occurring in the jumping spider's eye [20]. The new version of the EMD shown in figure 8 exploits the property of equation (2). The selective filters are centered arround 10Hz and the all-pass filter are used to compensate for the time-lag introduced by the negative phase of the selective filters. Considering equation (2), an edge gives a temporal frequency f_t = 10Hz while a bar gives f_t = 20Hz. In the first case (edge), two time-lag Δt_1 and Δt_2 will be available whereas in the second case (bar), only Δt_1 will be available. By comparing, Δt_1 with Δt_2, step 3 shown in figure 8 gives to the EMD a strong selectivity and thus, the ability to discriminate a bar from an edge, whatever the width of the bar.

3.4 Enlarging the Field-of-View (FOV)

Figure 9b shows an enhanced version of figure 1 where the local visual field $\Delta\varphi$ is replicated as many times as adjacent pixels. Imposing the micro-scanning movement upon the whole retina presents three main advantages :

- a large FOV can be obtained, depending on the size of the retina.
- a low resolution imager can be used because of the *hyperacuity* property (cf. section 3.2) wich will be retained within each local visual field $\Delta\varphi$. The only requirement is here to replicate all the signal processing steps (n-1) times for a retina containing n pixels.
- a custom-made 1D retina made of filiform photoreceptors (see figure 9a) can be used to improve the detection of cables.

Retina's shape adaptation to the type of objects that has to be detected is not a new principle. Male jumping spiders have been claimed to exploit largely the combination of such retinal micro-movements with an elongated retina to improve its capability to detect the legs of its female conspecific [20].

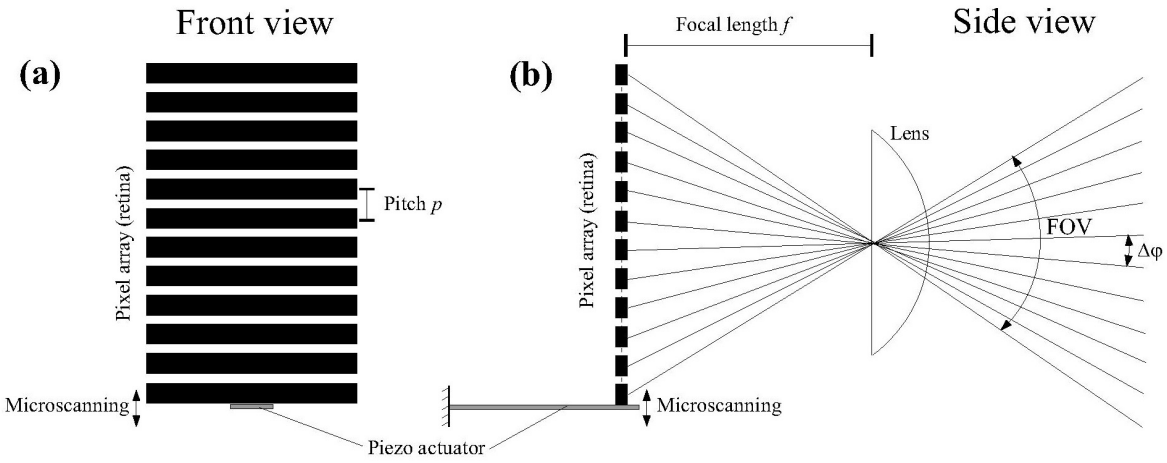

***Fig. 9**. (a) 1D retina made of filiform photoreceptors meant to improve the detection of horizontal lines (cables, wires…). (b) N pixels with (n-1) elementary local visual fields $\Delta\varphi$, can make for a large FOV while retaining the property of hyperacuity within each interreceptor angle $\Delta\varphi$.*

4 CONCLUSION

The detection system presented here is a proof-of-concept device aimed at non emissive, low cost, low weight and low power consumption powerline detection systems. The principle of this detection system relies on particular micro-movements imposed upon a retina made of infrared photodiodes. Our prototype was composed of a lens (focal length 80mm), an elementary retina (composed of only two elongated pixels) mounted at the tip of a piezo-actuator. On the basis of the retinal microscanning process that we identified several years ago in the fly compound eye [15], we made the piezo-actuator perform a periodic scanning movement at 10Hz. We have shown that the bio-inspired particular scanning law imposed to a retina mounted behind a fixed lens, overcomes classical optical limitations in terms of:

- *detection* beyond the resolution limit (*minimum visibile*). The system is able to see a thin bar of 0.3mm at a distance of 10m giving a potential detection of a cable of 3cm diameter at 1km.
- *localization* beyond the resolution limit (*hyperacuity*). The system can locate a contrasting object with a resolution 30 times better than the angular pitch $\Delta\varphi$.

By modifying an existing design of the EMD circuit, we integrated the ability to discriminate a bar (wire) from an edge (e.g, the horizon). The criteria implemented is entirely based on a fundamental property of the scanning process which transforms spatial frequencies of the scene into temporal frequencies at the photoreceptor level.
The width of the FOV of the detection system is a critical parameter because it should be large enough to detect objects that would interfere with reasonable flight trajectories. However, we have shown that the FOV can be increased by using one ore several off-the-shelf imagers or custom-made retinae with photoreceptors whose shape is in conformity with the object (cable) to be detected (Fig. 9). A similar scanning principle could be used for enhanced infrared goggles for helicopter pilots. In our approach where we take lessons from nature, we are working on the design of an 1D retina made of filiform photoreceptors to improve the capability to detect filiform objects. We are investigating achitectures based on FPGA to integrate all the signal processing steps of the detection system.

ACKNOWLEDGEMENTS

We are grateful to F. Ruffier for interesting comments, to M. Boyron, F. Paganucci and Y. Luparini for their involvement in the electronic and mechanical design. Special thanks are due to Dr Favennec, Dr J. Allard and Dr R. Piré from Eurocopter, Marignane, France, for their kind introduction to the field and issues related to powerline detection systems.

REFERENCES

[1] N. Yonemoto, K. Yamamoto, K. Yamada, H. Yasui, S. Nasu, H. Nebiya, C. Migliaccio and C. Pichot, “Obstacle detection and warning for helicopter flight using infrared and millimeter wave”, Proceedings of SPIE, Vol. 5081, 2003, pp 31-38.

[2] P. Avizonis and B. Barron, “Low cost wire detection system”, in Proc of IEEE Digital Avionics Systems Conference, vol. 1, 1999, pp. 3.C.3-1 - 3.C.3-4.

[3] K. R. Schulz, S. Scherbarth and U. Fabry, “Hellas : Obstacle warning system for helicopters”, Proceeding of SPIE, Vol. 4723, 2002, pp 1-8.

[4] R. J. Grasso, Adam C. P. Pratty, C. M. Vann, C. G. Stimson and J. E. Ackleson, “OASYS laser radar characterization of natural and manmade terrestrial features”, Part of the EUROPTO conference on commercial sensing platforms and applications, SPIE, Florence, Italy, 1999, pp 620-631.

[5] W. Koechner, “Wire obstacle avoidance system for helicopter”, United States Patent (patent number 4,902,126), 20 February 1990.

[6] B. Grossmann, A. Capbern, M. Defour and R. Fertala, A cable detection lidar system for helicopters, In NASA. Langley Research Center, 16th International Laser Radar Conference, Part 2 p 589-592 (SEE N92-31013 21-35), 1992.

[7] M. Zuta, “Wire detection system and method”, United States Patent (patent number 6,278,409), 21 August 2001.

[8] H. Essen, S. Boehmsdorff **,** G. Biegel and A. Wahlen, On the scattering mechanism of power lines at millimeter-waves, IEEE Transactions on Geoscience and Remote Sensing, 40 (2002) 1895 – 1903.

[9] A. Horridge, The spatial resolutions of the apposition compound eye and its neuro-sensory feature detectors : observation versus theory, J. of Insect Physiology, 51 (2005) 243-266.

[10] N. Franceschini and R. Chagneux, Repetitive scanning in the fly compound eye, in Göttingen Neurobiology Report, Thieme, Stuttgart, vol. 2, 1997, pp. 279.

[11] N. Franceschini, A. Riehle, and A. Le Nestour, Directionally Selective Motion Detection by Insect Neurons, *Facets of Vision*, pp. 360-390, eds. Stavenga & Hardie, Springer, Berlin, Germany, 1989.

[12] N. Franceschini, J. M. Pichon, and C. Blanes, From insect vision to robot vision, *Phil Trans Roy Soc Lond B* 337, pp. 283-294, 1992.

[13] N. Franceschini, S. Viollet and M. Boyron, Method and device for hyperacute detection of an essentially rectilinear contrast edge and system for line following and fixing of said contrast edge, Patent WO2005111536, 2005.

[14] F. Ruffier, S. Viollet, S. Amic, and N. Franceschini (2003), Bio-inspired optic flow circuits for the visual guidance of micro-air vehicles, IEEE ISCAS 2003, Bangkok, Thailande, pp. 846-849.

[15] S. Viollet, and N. Franceschini (1999), Visual servo system based on a biologically-inspired scanning sensor, *Sensor fusion and decentralized control in Robotics II*, G.T. McKee and P. Schenker (Eds.), SPIE vol. 3839, USA, ISBN 0-8194-3432-9, pp. 144-155.

[16] S. Viollet, and N. Franceschini (2001), Super-accurate visual control of an aerial minirobot, *Autonomous Minirobots for Research and Edutainment AMIRE*, U. Rückert, J. Sitte and U. Witkowski (Eds), Heinz Nixdorf Institute, Paderborn, Allemagne, ISBN 3-935433-06-9, pp. 215-224.

[17] N. Franceschini, K. Kirschfeld, Etude optique in vivo des éléments photorécepteurs dans l’oeil composé de *Drosophila* , Kybernetik, 8 (1971) 1-13.

[18] C. Martin, J. Lovberg, S. Clark and J. Galliano, ”Real time passive millimeter-wave imaging form a helicopter platform”, in: Proc of IEEE Digital Avionics Systems Conferences, vol. 1, 2000, pp. 2B1/1 - 2B1/8.

[19] O. Landolt and A. Mitros (2001) Visual sensor with resolution enhancement by mechanical vibrations. Autonomous Robots 11: 249-264

[20] M. F. Land (1972), Mechanisms of orientation and pattern recognition by jumping spiders (*Salticidae*), Information processing in the visual systems of arthropods, R. Wehner (ed.), Springer, Berlin, pp. 231-247.